Eur. Phys. J. C (2005)
Digital Object Identifier (DOI) 10.1140/epjc/s2005-02162-8

THE EUROPEAN PHYSICAL JOURNAL C

# How should we probe a strongly coupled quark–gluon plasma?

E. Shuryak[1,a]

Department of Physics and Astronomy, University at Stony Brook, NY 11794, USA

Received: 17 January 2005 /
Published online: 23 March 2005 – 

**Abstract.** Dramatic changes had occurred with our understanding of quark–gluon plasma, which is now believed to be rather strongly coupled. One set of questions is what is its internal structure: at the moment the best answer seem to be a liquid made of binary bound states. Another set of questions is how to probe it, especially using hard probes of the main interest to this meeting. Three suggestions to be discussed are (i) the ionization losses related to new bound states; (ii) the "conical flow" from quenched jets; (iii) possible new peaks in the dilepton spectra, corresponding to vector mesons above $T_c$.

**PACS.** 12.38.Mh, 25.75.-q

## 1 How strongly coupled is QGP?

Although some speculations about further running of the QCD coupling constant at $T > T_c$ to higher values were around for a while (see e.g. Fig. 5 in [1]) the convincing arguments for a different strong-coupling regime of QGP were
(i) the triumph of the collisional (hydrodynamical) description of particle spectra at RHIC, displaying strong radial and elliptic flows [2,3];
(ii) the discovery of multiple bound states of heavy and light quarks at $T > T_c$, from the lattice correlators [4] and directly from the Schroedinger/Klein–Gordon/Dirac equations [5,6] with proper lattice-based static potentials [8].

These general arguments are by now well accepted in the community, see e.g. [9] and the "experimental white papers", and so I would not return to them here.

Let me just comment on a few inevitable questions. The first one is obviously *How strong is strong enough?* The answer suggested in a "strong-coupling" paper by Zahed and myself [5] was that the effective interaction between quasiparticles should be sufficiently strong to create some *bound states* of the quasiparticles. The lines of *marginal states* with zero binding on the phase diagram fill the sQGP (strongly coupled QGP) region, and thus the last of those – presumably for the most attractive $gg$ singlet channel – serves as the boundary of sQGP. These lines are of course *not* singularities of the thermodynamical quantities, because as marginal states become virtual, the scattering amplitude remains continuous.

Below these lines the binary channels have non-zero binding. One particular case, important for QGP signals, is survival of $J/\psi$ as a bound state into the sQGP domain. According to our calculations based on lattice potentials [6] the critical temperature of its melting is around 2.5–$3T_c$. It is a bit higher than lattice results [4] using the MEM method, which is in fact consistent since lattice calculations are done in a relatively small volume. Thus, the observed charmonium suppression at SPS is not a Matsui–Satz "melting" but is due to some other mechanism, e.g. the "photo-effect" $gJ/\psi \to \bar{c}c$. The reason is that Debye–Huckel theory of screening, which demands *negative* correlation energy of a static charge in plasma, is only valid in weakly coupled plasma at very high $T$, while in sQGP the screening happens in a different way, by an $O(1)$ particle. The correlation energy (as deduced from the half-potential at large distances) is actually positive and large close to $T_c$. The reason for that, as well as for rather large quasiparticle masses for light quarks and gluons, are not yet understood.

Another logical consequence of the sQGP scenario described in detail in our second paper [6] is that at $T > T_c$ we expect approximate Casimir scaling of forces in all channels and thus hundreds of *colored* bound states, such as $(qg)_3$ and $(gg)_8$. This prediction is not yet tested on the lattice, but it should be. The calculations presented in this work also answer the "pressure puzzle", related to the question of how large pressure is generated by not-so-light quasiparticles. It was found that the addition of new binary states helps to get thermodynamics in line with lattice EoS. (Which also is experimentally tested via hydro and is shown to work.) The results [6] for masses and pressure for such a model are shown in Figs. 1 and 2.

This is of course only a beginning of the road toward a full understanding of sQGP. Studies related to 3-body physics (known as the Efimov effect) have revealed that if there are marginal 2-body states, there must also be 3-body ones, some of them even deeply bound. As really

[a] e-mail: shuryak@tonic.physics.sunysb.edu

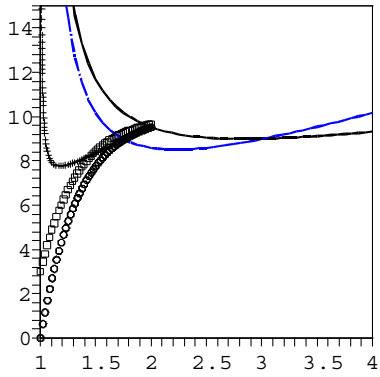


**Fig. 1.** The lines show twice the effective masses for quarks and gluons versus temperature $T/T_c$. Note that for $T < 3T_c$ $M_q > M_g$. Circles and squares indicate estimated masses of the pion-like and rho-like $\bar{q}q$ bound states, while the crosses stand for all colored states

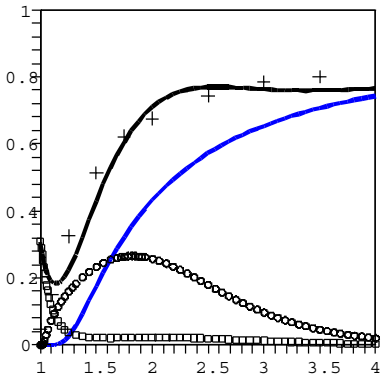


**Fig. 2.** Pressure (in units of that for a gas of massless and non-interacting quasiparticles) versus the temperature $T/T_c$. The crosses correspond to the $N_f = 2$ lattice results, from Fig. 2 of [7]. their uncertainty (not shown) is about 15 percent. The lower solid curve is the contribution of unbound quasiparticles, the upper includes also that of all bound states. Squares are for the pion-like and rho-like $\bar{q}q$ bound states combined, and circles for all the colored bound states

many-body studies are not yet done, it may well be that sQGP is polymerized into some chains, or crystallizes into a (locally ordered) liquid. Color degrees of freedom are numerous and provide lots of possibilities, so a lot of hard work is ahead to understand the sQGP structure.

As experience of other fields shows, global EoS is probably too insensitive a measure to tell the difference between all those models, at least with the level of accuracy we now have. *Transport properties* like *viscosity* are a different matter; they are known to be quite sensitive to coupling and can vary by several orders of magnitude for known liquids and plasmas. Its theory is still missing, and a lot of efforts would be needed to have it.

One early idea suggested in [5] is based on the *marginal states* with small binding, which may be related to large scattering length and hydro behavior.

This idea is further confirmed by experiments with cold atoms, where precisely this mechanism – known as the Feshbach resonance – is used. Not only the elliptic flow in agreement with hydrodynamics was observed [10], but more recent experiments such as [11] have revealed that in fact the frequency of the two lowest ($z$- and $r$-modes) of oscillations in an elliptic trap both agree with the hydro prediction to better than a percent. Furthermore, the damping-to-frequency ratio dives from $\sim .1$ to about $10^{-3}$ near the Feshbach resonance. It means that there hydro oscillations may be repeated about a thousand times, before dissipative viscose effects take over and kill it. And all of it happens, let me repeat, where the interaction is the *strongest*, corresponding to viscosity as strikingly small [12], as it is for QGP at RHIC.

Another connection on which I would like to provide an update is a connection to $\mathcal{N} = 4$ SUSY YM theory and the AdS/CFT correspondence. Let me just recall that this theory has zero beta function and the coupling does not run, and for all values from 0 to infinity the finite-$T$ version of it is in the same Coulomb (QGP-like) phase. So it is a perfect theoretical laboratory, telling us what all quantities are in the limit of very strong coupling. In [13] we argued that matter is made not from quasi-particles, which have large masses $M_{q,g} \sim \sqrt{\lambda}T$ (where $\lambda = g^2 N_c >> 1$ is the 't Hooft gauge coupling) but of deeply bound binary states of those with much smaller masses $M_{\rm mesons} \sim T$ which we found for relativistically rotating states with large angular momentum. Recently there was a progress in introducing fundamental massive quarks into AdS/CFT theory, living on a separate D7 brane, with results for "charmonium" spectroscopy in strong coupling [14]. It was found that rotating states are light, but their masses $M_{\rm mesons} \sim M_q/\lambda^{1/4}$, while the "s-wave" states with zero orbital momentum do not "fall on the center" but survive and do have even smaller masses $M_{\rm mesons} \sim M_q/\lambda^{1/2}$, the same scale as advocated in our paper. Thus the splitting between $J/\psi, \eta_c$ and $\chi$ states is large and parametric in the strong coupling. It remains to be seen what happens with strongly coupled charmonium at finite $T$, a question which is to be resolved next.

## 2 Where does the energy of the quenched jets go?

Quenching of high-$p_t$ QCD jets observed at RHIC imply deposition of a large fraction or even all their energy into matter. If it is sQGP, argued to be a near-perfect liquid, this energy should not dissipate but propagate outward as a "conical flow" similar to well known sonic booms from supersonic planes. This idea is developed in a recent paper [15], on which this section is based.

In what follows, we would like to treat separately two different types of energy losses:
(i) the *radiative* losses, producing mostly relativistic gluons and
(ii) the *scattering/ionization* losses, which deposit energy in the medium. Radiative losses [16,17] are the dominant mechanism. However both the primary parton and radiated gluons move with about the same speed (the speed of

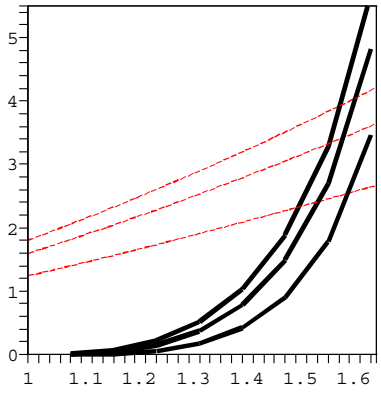


**Fig. 3.** Gluon energy loss $\mathrm{d}E/\mathrm{d}x$ in GeV/fm versus the temperature $T/T_\mathrm{c}$ (in units of the critical one). The thick solid lines are for the "ionization" losses, while the thin dashed lines are for the elastic losses. In each set the three curves from top to bottom are for a gluon with energy 15, 10 and 5 GeV

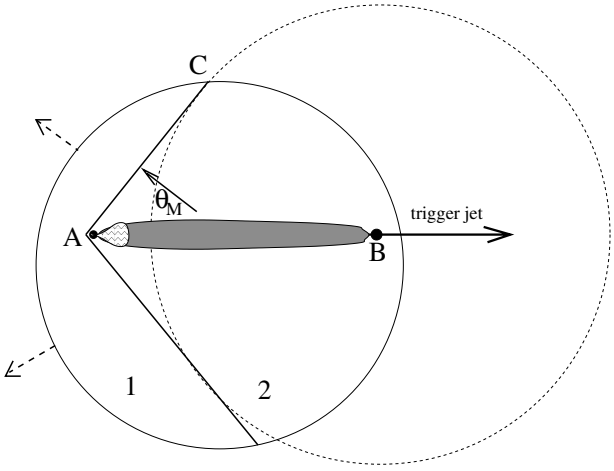


**Fig. 4.** A schematic picture of flow created by a jet going through the fireball. The trigger jet is going to the right from the origination point (the black circle at point B) from which sound waves start propagating as spherical waves (the dashed circle). The companion quenched jet is moving to the left, heating the matter and thus creating a cylinder of additional matter (shaded area). The head of the jet is a "non-hydrodynamical core" of the QCD gluonic shower, formed by the original hard parton (black dot A). The solid arrow shows a direction of flow normal to the shock cone at the angle $\theta_\mathrm{M}$; the dashed arrows show the direction of the flow after the shocks hit the edge of the fireball

light) so from the viewpoint of matter those can be treated as one external object. What is now more important are elastic energy losses (first studied by Bjorken [18]) and also those due to "ionization" of new bound states in sQGP. The latter contribution was recently calculated by Zahed and myself [19]. These mechanisms deposit additional energy, momentum and entropy into the matter; see Fig. 3. It is their combined magnitude, $\mathrm{d}E/\mathrm{d}x = 2$–$3\,\mathrm{GeV/fm}$, which we will use below. Even at such loss rates, a jet passing through the diameter of the fireball, created in central Au+Au collisions, should deposit up to 20–30 GeV, enough to absorb jets of interest at RHIC.

Let us start a discussion of associated collective effects with *the energy scales involved*. While the total CM energy in a Au+Au collision at RHIC is very large, about 40 TeV, compared to the energy of a jet (typically 5–20 GeV), the jet energy is transverse. The total transverse energy of all secondaries per one unit of rapidity $\mathrm{d}E_\perp/\mathrm{d}y \sim 600\,\mathrm{GeV}$. Most of it is thermal, with only about 100 GeV being related to collective motion. Furthermore, the so called elliptic flow is a $\sim 1/10$ asymmetry and therefore it carries an energy of $\sim 10\,\mathrm{GeV}$ which is quite comparable to that lost by the jets in question. Since elliptic flow was observed and studied in detail, we conclude that conical flow should be observable as well. (In order to separate the two, it is beneficial to focus first on the most central collisions, with the elliptic flow is as small as possible.)

Figure 4 explains a view of the process, in a plane transverse to the beam. Two oppositely moving jets originate from the hard collision point B. Due to strong quenching, the survival of the trigger jet biases it to be produced close to the surface and to move outward. This in turn forces its companion to move inward through the matter and to be maximally quenched.

The energy deposition starts at point B; thus a spherical sound wave appears (the dashed circle in Fig. 4). Further energy deposition is along the jet line and is propagating with the speed of light, till the leading parton is found at point A at the moment of the snapshot. As is well known, the interference of perturbations from a supersonically moving body (such as a supersonic jet plane or meteorite) creates conical flow behind the shock waves. The angle $\theta_\mathrm{M}$ defined in the figure is given by a simple geometrical condition: distance $\mathrm{AB} = ct$ while $\mathrm{CB} = v_\mathrm{shock}t$. Apart from the region close to the head of the object, the shock waves are weak and thus they move with the speed of sound $v_\mathrm{shock} \approx c_\mathrm{s}$, and therefore

$$\cos\theta_\mathrm{M} = c_\mathrm{s}/c. \qquad (1)$$

(Below we will use units in which $c = 1$.) Since the velocity of the shock depends on its intensity, the cone should in fact be somewhat rounded near its top: that is ignored in the figure. Respectively the perturbations of the matter pressure and velocity $\delta p, \delta u$ becomes small at large $r$ and can be described in linear approximation

The region near the head of the jet, which we would refer to as a "non-hydrodynamical core", which is constantly producing gluons, which emits new ones etc.: the whole shower is a complicated non-linear phenomenon which should obviously be treated via the tools of quantum field theory. The energy/momentum flow through the core boundary we will treat phenomenologically, identifying it with $\mathrm{d}E/\mathrm{d}x$ of the second type, which we will approximate by a time-independent constant. This should thus lead to stationary-state conical flow, depending on $x - t$ only.

A shaded region in Fig. 4 consists of "new matter" related to the entropy produced in the process $\mathrm{d}S/\mathrm{d}x$, which can be calculated only with dissipative dynamics in the near zone, which we do not attempt in this work. Matter is expected to get equilibrated soon, and thus the radius of the cylinder $R_\mathrm{c}$ of new matter can be related by

$\mathrm{d}S/\mathrm{d}x = s(T)\pi R_c^2$. As is well known, the constant size cylinder does not emit any sound.

*Hydrodynamical equations* we use are linear since the whole energy deposited by the jets can be treated as small compared to the total energy of the medium. We will use cylindrical coordinates with $x$ along the jet axis and $r$ orthogonal to it.

For simplicity we will assume that the perturbed medium is homogeneous and at rest. In this linearized approximation the non-zero components of the stress-energy tensor are

$$\delta T^{00} = \delta\epsilon, \quad \delta T^{0i} = (\epsilon + p)v^i, \quad \delta T^{ij} = \delta p \delta^{ij}, \quad (2)$$

where $\epsilon$ and $p$ are the internal energy and pressure and $\boldsymbol{v}$ is the velocity field of the perturbation. Thus, by recalling that $\frac{\partial p}{\partial e} = c_s^2$ (with $c_\mathrm{s}$ the velocity of sound) the energy and momentum conservation equation $\partial_\mu \delta T^{\mu\nu}$ can be written as

$$\begin{aligned} \partial_0 \delta T^{00} + \partial_i \delta T^{0i} &= 0, \\ \partial_0 \delta T^{0i} + c_s^2 \partial_i \delta T^{00} &= 0. \end{aligned} \quad (3)$$

The initial conditions are set by the process of thermalization of the energy lost by the jet. As already mentioned, this thermalization process is very complicated and should take place at distances of the order $\Gamma_s$ from the production point. As $\Gamma_s$ is also the typical size of the liquid cells, we will simply consider that there is a variation of the energy and momentum at the position of the particle.

This initial condition can be easily expressed if we first concentrate in the perturbation due to the propagation of the particle in an interval $\mathrm{d}t$ around its position. In this case the previous conditions lead to

$$\begin{aligned} \delta T^{00}(t_0, x) &= \Delta E \delta^3(\boldsymbol{x}(t_0) - \boldsymbol{x}), \\ \delta T^{0x}(t_0, x) &= \Delta P \delta^3(\boldsymbol{x}(t_0) - \boldsymbol{x}), \end{aligned} \quad (4)$$

where we have assumed that the particle moves in the $x$ direction at the speed of light ($c = 1$) and $\boldsymbol{x}(t)$ is the trajectory of the particle ($x = t$). We assume also that the energy and momentum loss are equal and, as we look for a constant drag, we set $\Delta E = \frac{\mathrm{d}E}{\mathrm{d}x}\mathrm{d}t$. Assuming that $c_\mathrm{s}$ is constant, it can be shown that the solution for these conditions is given by

$$\begin{aligned} \delta T^{00} = \frac{1}{c_\mathrm{s}} \frac{\mathrm{d}E}{\mathrm{d}x} \mathrm{d}t_0 \left(\partial_t - \partial_x\right) \Theta(t - t_0) \\ \times \frac{\left[\delta\left(R - c_\mathrm{s}(t - t_0)\right) - \delta\left(R + c_\mathrm{s}(t - t_0)\right)\right]}{4\pi R}, \end{aligned} \quad (5)$$

where $R = |\boldsymbol{x} - \boldsymbol{x}(t_0)|$, the distance from the observation point to the emission point at the intersection of the past "sound cone" and a jet world line. The reader can readily identify the argument of the derivatives as the retarded Green's function of the wave equation and should be warned that $R$ depends on observation time and space point. The calculation is close to that done for electromagnetic waves (Cerenkov radiation), except that sound is a longitudinal excitation.

In general, let a jet be born at the initial point $t_\mathrm{i}$ and die at the final point $t_\mathrm{f}$. A point-like source creates two spheres of perturbation, with the Mach cone tangent to both:

$$\begin{aligned} \delta T^{00} \\ = \frac{1}{c_\mathrm{s}^2} \frac{\mathrm{d}E}{\mathrm{d}x} \left( \frac{\delta(t - t_\mathrm{i} - R_{t_\mathrm{i}}/c_\mathrm{s})}{4\pi R_{t_\mathrm{i}}} - \frac{\delta(t - t_\mathrm{f} - R_{t_\mathrm{f}}/c_\mathrm{s})}{4\pi R_{t_\mathrm{f}}} \right) \\ - \frac{2}{c_\mathrm{s}^2} \frac{\mathrm{d}E}{\mathrm{d}x} \partial_x \frac{\Theta(t - t_\mathrm{i} - R(t)/c_\mathrm{s}) \Theta(t_\mathrm{f} - t + R(t)/c_\mathrm{s})}{4\pi \sqrt{(x - t)^2 - \left(\frac{1}{c_s^2} - 1\right) r^2}}; \end{aligned} \quad (6)$$

when integrating over the whole space, the two spherical terms give the total deposited energy $\frac{\mathrm{d}E}{\mathrm{d}x}(t_\mathrm{f} - t_\mathrm{i})$. The conical term apparently has no energy. In order to explain why, we prefer to regularize the problem, introducing a distributed source, e.g. a Gaussian one, see the paper for details.

*How can the effect be observed?* The most important feature of conical flow is its direction, which is normal to the shock front and thus making the so called Mach angle (1) with the jet direction, determined basically by the speed of sound in matter. So one can conclude that quenched jets must be accompanied by a cone of particles with the opening angle $\theta_\mathrm{M}$. This cone angle should be the same for any jet energy (in contrast to radiation angles which are shrinking at high energy).

Let us start with the simplest case of central collisions, in which the cross section of the fireball is a circle and the elliptic flow is absent. Most quenched jets going through it will pass a length comparable to its diameter, and thus the high-energy jets which are not quenched completely and reach through the fireball will produce conical flow during time $t \sim 10$–$15\,\mathrm{fm}/c$. At such a late time, the appropriate value for the speed of sound would correspond to matter being a "resonance gas", $c_\mathrm{s}^2 \approx .2$. We thus conclude that in this case the emission angle of the conical flow should be at the angles (relative to trigger)

$$\theta_\mathrm{emission} = \pi \pm \arccos(c_\mathrm{s}/c) \approx 2.0, 4.2. \quad (7)$$

In Fig. 5 we show preliminary data from the STAR experiment (another RHIC experiment, PHENIX, sees a similar distribution which is too recent to be released at this point). The upper figure corresponds to *pp* collisions and the lower to central Au + Au ones. The peak near angle zero consists of particles from a triggered outward moving jet, while particles from the companion jet should result in a peak near $\Delta\phi = \pi$. Such a peak is clearly seen in *pp* collisions, in which no matter is present: but in Au + Au collisions one finds instead a *double-peaked* distribution with a *minimum* at the original jet direction, $\Delta\phi = \pi$.

Remarkably, as Fig. 5b shows, this value, $\pi \pm 1.1$, nicely agrees with the observed positions of the two maxima of the distribution of the secondaries, relative to the direction of the triggered hard charged hadron. Fortunately, in the experimental conditions the inward-moving jet is so completely quenched that presumably no contribution from the "non-hydro core" makes it to the opposite surface. Unfortunately, the angle versus which the distribution is plotted is not a polar angle with respect to the

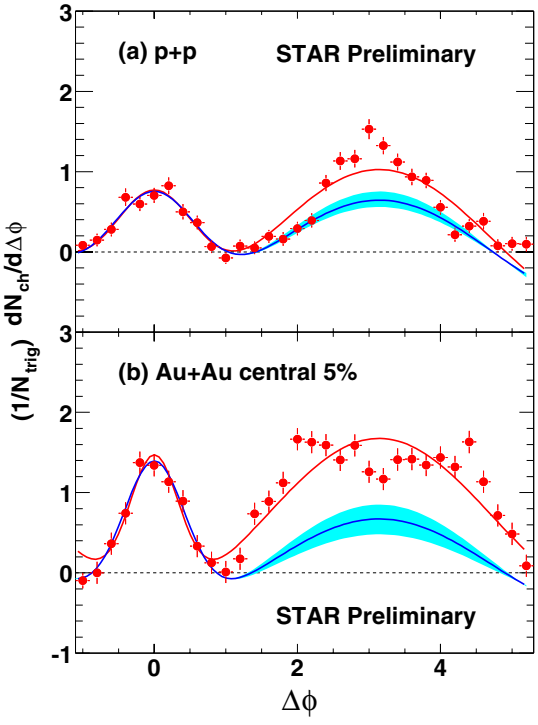


**Fig. 5.** The background subtracted distribution of secondaries in azimuthal angle $\Delta\phi$ which are associated with triggered hard charged hadron $p_t > 4\,\mathrm{GeV}$, by STAR collaboration [21]. **a** is for $p+p$ and **b** for 5% most central $\mathrm{Au}+\mathrm{Au}$ collisions

jet, $\theta$, but only a difference in their azimuthal angles, $\Delta\phi$, which reduces the effect.

Since the speed of sound is expected to change significantly during the fireball lifetime (from $c_s^2 = 1/3$ during the early QGP stage, to small values in the "mixed phase", and then to $c_s^2 \approx .2$ in the hadronic resonance gas), the Mach angle will depend on time and space as well. This feature can potentially be used to measure the speed of sound at different stages of the collisions.

## 3 Direct observation of binary bound states in sQGP via dileptons?

To use photons and dileptons as "penetrating probes" in order to get information about the earlier stages of heavy-ion collisions was one of the first suggestions to study the quark–gluon plasma (QGP) [22]. It was then argued that the invariant mass ($M^2 = (p_{l+} + p_{l-})^2$) spectra of penetrating probes produced in QGP should be monotonously decreasing with the dilepton mass, while those originating from hadronic matter at $T < T_c$ should instead show invariant mass peaks due to a familiar vector meson $\rho, \omega, \phi, J/\psi, ...$

With the advent of the sQGP regime, the logic of it is reversed [20]. If the meson-like bound states continue to exist at $T = (1\text{–}2)T_c = 170\text{–}350\,\mathrm{MeV}$ (the temperature range corresponding to QGP at RHIC), one expects to see them in dilepton spectra as well. Those should be rather heavy, although still below twice the effective quark quasiparticle mass.

Furthermore, even at higher $T$ when there are no bound states, there exists a near-threshold enhancement which may still be used to infer the value of the quasiparticle masses and the strength of their interaction.

Dileptons produced by vector resonances ($\rho, \omega, \phi, J/\psi$) are described by the first expression in (9), which can exist both in the hadronic phase and in sQGP. The dileptons are supposed to be the main part of the RHIC program: PHENIX was aimed at that from the beginning, and now also the STAR detector has an electromagnetic calorimeter. Large-statistics Run-4 data are now being analyzed, and the only published data so far concern PHENIX single electron production which is presumably dominated by charm decays.

Matter modification of more narrow $\omega, \phi$ resonances can obviously be observed only for a fraction of these particles decaying inside the fireball. Resonances decaying after freeze-out have the usual vacuum mass, and these decays produce a large "hadronic background" for such measurements: in fact the first dilepton experiment which has sufficient resolution to observe these modifications is NA60. However for sQGP vector mesons the mass modification is very large, e.g. we will discuss below peaks with masses up to $M \sim 1.5\text{–}2\,\mathrm{GeV}$, and so in this case the resolution is not so much an issue. Since $T$ changes during cooling, the masses of the peaks change with time and one may wonder if the very existence of the peaks can be observed. We hope it can be done in two *endpoints* mass regions:
(i) $M \sim 1.5\text{–}2\,\mathrm{GeV}$ corresponding to $T \approx T_{zb}$ (zero binding) and the edge of the quasiparticle continuum, at the initial QGP at RHIC;
(ii) $M \sim 0.5\,\mathrm{GeV}$, where we expect to see the contributions of the modified vector mesons at $T \approx T_c$.

Let us start with the basic expression for the dilepton production rate

$$\frac{\mathrm{d}R(T)}{\mathrm{d}^4x\mathrm{d}^4q} = \frac{\alpha^2}{48\pi^4}\frac{1}{\mathrm{e}^{\frac{q_0}{T}}-1}F, \tag{8}$$

where $\alpha$ is the electromagnetic coupling, $q_0$ is the dilepton energy and the "formfactors" $F$ for two well-tested processes are

$$F = \begin{cases} F_H \stackrel{\mathrm{def}}{=} \dfrac{m_\rho^4}{[(m_\rho^2 - M^2)^2 + m_\rho^2\Gamma_\rho^2]} & (\rho), \\ F_Q \stackrel{\mathrm{def}}{=} 12\sum_q e_q^2\left(1+\dfrac{2m_q^2}{M^2}\right)\left(1-\dfrac{4m_q^2}{M^2}\right)^{\frac{1}{2}} & (\mathrm{wQGP}), \end{cases} \tag{9}$$

where the former one corresponds to $\pi\pi \to \rho \to l^+l^-$ annihilation in a vacuum or hadronic phase at small $T$, written in standard vector-dominance form. The latter expression corresponds to $\bar{q}q$ annihilation similar to the partonic Drell–Yan process. If one ignores quark masses in $F_Q$, it is just a sum of squared charges for all relevant quarks, $u, d, s$ of all colors. This basic case we will use as our "standard candle" below, normalizing all predictions to the "standard wQGP rate" with $F_{\mathrm{wQGP}} = 24$. Detailed

calculations of the final dilepton spectra for such a "standard candle" model were done by Rapp and Shuryak [23] (including specific acceptance of the SPS NA50 experiment) and for RHIC by Rapp [25]. For a review see [26].

In terms of the imaginary part of the photon self-energy the wQGP limit means

$$\Im\Pi_{\rm em} = -\frac{M^2}{12\pi} N_c \sum_{q=u,d,s} (e_q^2). \tag{10}$$

If quark quasiparticles in the QGP phase are not massless (and current lattice calculations indicate they are as heavy as 1 GeV in the region of interest, $T_{\rm c}$–$3T_{\rm c}$) one would like to correct for that using the formulae from above. This fact leads to a trivial modification to the previous expression (that is relevant in the IMR):

$$\Im\Pi = \begin{cases} 0 \quad (M^2 < 4m_q^2), \\ \dfrac{-M^2}{12\pi} N_c \sum\limits_q e_q^2 \left(1+\dfrac{2m_q^2}{M^2}\right)\left(1-\dfrac{4m_q^2}{M^2}\right)^{\frac{1}{2}} \\ \quad (M^2 > 4m_q^2). \end{cases} \tag{11}$$

Furthermore, we expect a non-trivial modification of the annihilation cross section of quarks into leptons due to the attractive interaction between them. This modification will be specially important for near-threshold production, where we will use non-relativistic Green's functions. Modifications of the rates are also expected due to the presence of bound states, where, as we will see, the problem is intrinsically relativistic.

The basic idea is very simple: the probability of the $\bar{q}q \to l^+l^-$ process is enhanced by the initial state attractive interaction. Attractive interaction obviously correlates $\bar{q}$ and $q$ in space and increases the chances to find $\bar{q}q$ close to each other and annihilate. In such a general form, the enhancement persists whether the potential is deep enough to make bound levels or not, and whether quark quasiparticles have small or large width.

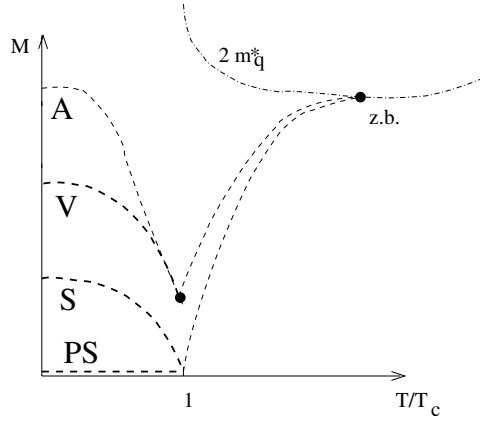


**Fig. 6.** Schematic $T$-dependence of the masses of $\bar{q}q$ states. $A, V, S$ and $PS$ stand for axial, vector, scalar and pseudoscalar states. The dash-dotted line shows the behavior of twice the quasiparticle mass. Two black dots indicate places where we hope the dilepton signal may be observable

In the case of a pure Coulomb interaction this phenomenon is well studied. The relevant parameter $z = \pi\alpha/v$ contains the ratio of the coupling strength to velocity, and the enhancement is in this case given by the well known Gamow factor[1]

$$F_{\rm Gamow} = \frac{z}{1-\exp(-z)}. \tag{12}$$

Note that the result is $\sim 1/v$ at small $v$ (large $z$) and 1 at small $z$. It cancels the velocity in the phase space and makes the production rate to jump to a *finite* value at the threshold.

A good example of the QCD-based color–Coulomb enhancement is the cross section for the production of the top quark pair $\bar{t}t$ [27,28]. The enhancement calculated in these works is found to be quite significant, in spite of the fact that the rather large width of the top quarks precludes them from forming topponium bound states. We used methods developed in these works, calculating Green's functions for lattice-based potentials.

The new (sQGP) part of this picture is at $T > T_{\rm c}$, which starts and ends at the points marked by small black circles. At any given $T$ there are two peaks in the spectral density, corresponding to invariant masses of the T, L components. On top of that, there is a threshold bump at $2m_q^*(T)$, which exists even at a $T$ so high that no bound states exists. Unfortunately, one can only observe a signal integrated over the expanding fireball, or over all temperatures involved between the initial and freeze-out ones. The integral tends to wipe out peaks at intermediate locations, unless there are special reasons for them to survive. Two of the black dots, at the mixed phase $T = T_{\rm c}$, have the benefit of a long time spent there during expansion. The same is true for the third black point, due to the near-constancy of the mass of weakly bound states at $T = 1.5$–$2T_{\rm c}$. The near-threshold bump is at about the same location at higher $T$ as well. Thus one may hope (and we will show it below) that the structures corresponding to these endpoints (black circles at Fig. 6) may be detected.

Although at finite temperatures and non-zero momentum relative to heat bath are split into distinct longitudinal and transverse (L, T) modes, those should coincide at zero momentum. Since all masses are large compared to the relevant $T$ at the time, only pairs with small momentum are actually produced. Furthermore, lattice experience of similar quasiparticle modes indicates that they follow, at least approximately, the vacuum-like dispersion law $\omega^2 = p^2 + M^2$, and so using the invariant mass rather than energy would take care of canceling the momentum dependence.

In Fig. 6 we have shown only states made of $u, d$ quarks, ignoring the strange one. Needless to say, those exist and can be also produced. The peaks of $\bar{s}s$ $\phi$-like states should be shifted in mass upward by $2m_s \approx 250$–$300\,{\rm MeV}$, but their contribution to dilepton spectra is proportional

[1] The sign in exponent is the opposite to that on the original Gamow factor, for the alpha-particle interaction with nuclei, or that used for HBT correlations, corresponded to a *repulsive* Coulomb force.

to the square of the electric charge $q_s^2 = 1/9$, which is three times smaller than the average of $q_u^2 = 4/9, q_d^2 = 1/9$. Strange states are more promising for pseudoscalar/scalar signals, to which we turn below.

In [28] the cross section $\sigma(e^+e^{\rightarrow}t\bar{t})$ is analyzed to leading-logarithmic order in QCD in the *non-relativistic limit* (close to threshold). The main result, already used in [27], is the modification of the threshold factors from the well known leading order expression

$$\sigma_{\rm LO} = \frac{4\pi\alpha_{\rm QED}^2 e_t^2}{3s} N_c \sqrt{\left(1-\frac{4m_t^2}{s}\right)}\left(1+\frac{2m_t^2}{s}\right) \quad (13)$$

to

$$\sigma = \frac{4\pi\alpha_{\rm QED}^2 e_t^2}{3s} N_c \frac{24\pi \Im G_{E+{\rm i}\Gamma_t}(0,0)}{s}, \quad (14)$$

where $E$ is the center of mass energy and $\Gamma_t$ is the width of the top quark (related to the lifetime due to weak decays). The relation for the dilepton production rate is obtained by obvious substitution of $\Im G/s$ into $F_Q$ in (9).

As a further clarification, in the limit $\Gamma = 0$ we can rewrite

$$\Im G_{E+{\rm i}0^+}(0,0) = \sum \psi_n(0)\psi_n(0)^\dagger \delta(E_n - E). \quad (15)$$

Note that the sum runs over *all* states, including scattering states, where the sum should be replaced by an integral. This expression explains quite clearly the connection between the Green's function and the standard non-relativistic formula for the annihilation of bound states and (15) gives the flux factor that multiplies the annihilation cross section at zero momentum:

$$\frac{1}{\tau_{\rm lifetime}} = \sigma_{q\bar{q}}(s=4m_q)|\psi_n(0)|^2. \quad (16)$$

The non-relativistic Green's function $G_{E+{\rm i}\Gamma_t}(r,\bar{r})$ obeys the usual Schroedinger equation:

$$\left[-\frac{1}{m}\boldsymbol{\nabla}^2 + V(\boldsymbol{r}) - (E+{\rm i}\Gamma)\right] G_{E+{\rm i}\Gamma}(r,\bar{r}) = \delta^3(\boldsymbol{r}-\bar{\boldsymbol{r}}), \quad (17)$$

with inter-particle potential $V(\boldsymbol{r})$. Analytic expressions for the Green's function for the pure Coulomb potential are well known; see e.g. [27]. For a realistic lattice-based potential we will use a numerical method following [28], which is valid for all potentials less singular than $1/r^2$. The benefit of it is that one avoids summations over levels, and bound states are automatically included together with scattering ones. As a test, we checked that it reproduces well known results for the Coulomb potential with an accuracy of at least a few per mill.

Let us now explain our units. Since the effective mass of the quark quasiparticle in the temperature interval considered is not known accurately, we use it as our basic energy unit. In plots twice this value appears as a threshold, to which we tentatively ascribe the particularly simple value $2M_q = 2\,{\rm GeV}$: the reader should however be warned that this is a "GeV" in quotation marks, to be rescaled appropriately later when the value of the quark effective masses in QGP will be better known.

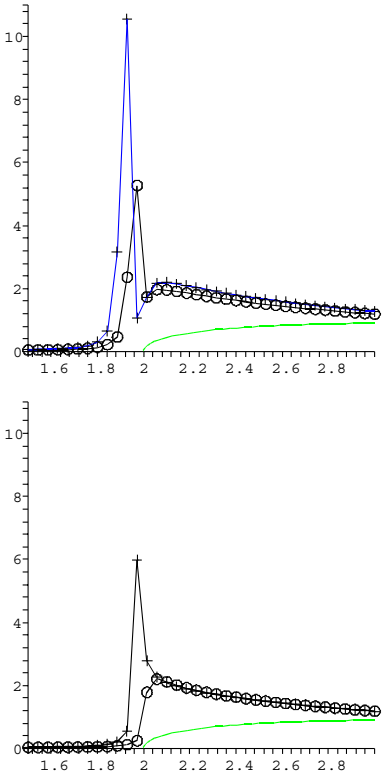


**Fig. 7.** Modification of the spectral density versus the invariant mass in $M_q$ units for different temperatures: **a** $1.2\,T_{\rm c}$ (cross) and $1.4\,T_{\rm c}$ (circle), **b** $1.7\,T_{\rm c}$ (cross) and $3\,T_{\rm c}$ (circle) and the correction due to quark mass (line)

What we learned from these calculations is how the spectral density changes as the bound states become less and less bound until the system arrives at zero binding (zero binding point). In Fig. 7 we show the shape of the dilepton spectral density for different temperatures ($1.2T_{\rm c}$, $1.4T_{\rm c}$, $1.7T_{\rm c}$, $3T_{\rm c}$). One can observe how exactly enhancement in the bound state and threshold region changes. The height of this enhancement depends on the proximity of the level; at $1.7T_{\rm c}$, where the bound level is close to threshold, we observe a big modification of the spectral function at 2 GeV. Note that proximity of the level to threshold happens in a rather wide $T$ interval, roughly between $1.5T_{\rm c}$ to $2T_{\rm c}$ (the zero binding point [5]). Note also that the enhancement is still seen at temperatures as high as $3T_{\rm c}$, when all bound states have already been melted.

The issue of the observability of these peaks depends on their width: its magnitude is being addressed right now and I am not yet ready to report those. The pictures above only have "numerical width" for plotting, and thus are not realistic. However it is very likely that the width is not overwhelming to preclude their observation.

*Acknowledgements.* I am thankful to the organizers, especially to Helmut Satz and Carlos Lorenco, for making this important conference at such a nice location possible. The results reported in the talk were obtained with my collaborators G. Brown, J. Casalderrey-Solana, D. Teaney and I. Zahed. This work was partially supported by the US-DOE grants DE-FG02-88ER40388 and DE-FG03-97ER4014.

## References

1. E. Shuryak, Nucl. Phys. A **715**, 289 (2003) [hep-ph/0205031]
2. D. Teaney, J. Lauret, E.V. Shuryak, Phys. Rev. Lett. **86**, 4783 (2001) [nucl-th/0011058]; A hydrodynamic description of heavy ion collisions at the SPS and RHIC, nucl-th/0110037
3. P.F. Kolb, P. Huovinen, U. Heinz, H. Heiselberg, Phys. Lett. B **500**, 232 (2001). More details in P.F. Kolb, U. Heinz, in Quark Gluon Plasma 3 (edited by R.C. Hwa, X.N. Wang), nucl-th/0305084
4. M. Asakawa, T. Hatsuda, Nucl. Phys. A **715**, 863c (2003); S. Datta, F. Karsch, P. Petreczky, I. Wetzorke, Nucl. Phys. B (Proc. Suppl.) **119**, 487 (2003) [hep-lat/0208012]
5. E.V. Shuryak, I. Zahed, Phys. Rev. C **70**, 021901 (2004) [hep-ph/0307267]
6. E.V. Shuryak, I. Zahed, Phys. Rev. D **70**, 054507 (2004) [hep-ph/0403127]
7. F. Karsch, E. Laermann, A. Peikert, Phys. Lett. B **478**, 447 (2000)
8. O. Kaczmarek, S. Ejiri, F. Karsch, E. Laermann, F. Zantow, Prog. Theor. Phys. Suppl. **153**, 287 (2004) [hep-lat/0312015]. See also talks by F. Karsch, P. Petreczky in these proceeedings
9. M. Gyulassy, L. McLerran, nucl-th/0405013
10. K.M. O'Hara et al., Science **298**, 2179 (2002); T. Bourdel et al., Phys. Rev. Lett. **91**, 020402 (2003)
11. M. Bartenstein et al., cond-mat/0403716
12. B.A. Gelman, E.V. Shuryak, I. Zahed, nucl-th/0410067
13. E.V. Shuryak, I. Zahed, Phys. Rev. D **69**, 014011 (2004) [hep-th/0308073]
14. M. Kruczenski, D. Mateos, R.C. Myers, D.J. Winters, JHEP **0307**, 049 (2003) [hep-th/0304032]; S. Hong, S. Yoon, M.J. Strassler, JHEP **0404**, 046 (2004) [hep-th/0312071]
15. J. Casalderrey-Solana, E.V. Shuryak, D. Teaney, hep-ph/0411315
16. M. Gyulassy, M. Plumer, Phys. Lett. B **243**, 432 (1990); X.N. Wang, M. Gyulassy, M. Plumer, Phys. Rev. D **51**, 3436 (1995); G. Fai, G.G. Barnafoldi, M. Gyulassy, P. Levai, G. Papp, I. Vitev, Y. Zhang, hep-ph/0111211
17. R. Baier, Y.L. Dokshitzer, S. Peigne, D. Schiff, Phys. Lett. B **345** (1995); R. Baier, Y.L. Dokshitzer, A.H. Mueller, D. Schiff, JHEP **0109**, 033 (2001)
18. J.D. Bjorken, FERMILAB-PUB-82-059-THY; D.A. Appel, Phys. Rev. D **33**, 717 (1986); J.P. Blaizot, L.D. McLerran, Phys. Rev. D **34**, 2739 (1986)
19. E.V. Shuryak, I. Zahed, Ionization of binary bound states in a strongly coupled quark–gluon plasma, hep-ph/0406100
20. J. Casalderrey-Solana, E.V. Shuryak, hep-ph/0408178
21. Fuqiang Wang for STAR collaboration (Quark Matter 2004), J. Phys. G **30**, 1299 (2004); nucl-ex/0404010
22. E.V. Shuryak, Phys. Lett. B **78**, 150 (1978), Yadernaya Fizika (Sov. J. Nucl. Physics) **28**, 796 (1978); Phys. Rep. **61**, 71 (1980)
23. R. Rapp, E.V. Shuryak, Phys. Lett. B **473**, 13 (2000)
24. B. Kämpfer, K. Gallmeister, O.P. Pavlenko, hep-ph/0102192; Phys. Lett. B **473**, 20 (2000)
25. R. Rapp, Thermal lepton production in heavy-ion collisions, nucl-th/0204003; see also hep-ph/0201101
26. R. Rapp, J. Wambach, Adv. Nucl. Phys. **25**, 1 (2000) [hep-ph/9909229]
27. V.S. Fadin, V.A. Khoze, Sov. J. Nucl. Phys. **48**, 309 (1988) [Yad. Fiz. **48**, 487 (1988)]
28. M.J. Strassler, M.E. Peskin, Phys. Rev. D **43**, 1500 (1991)